

A Low Shear Viscometer with Automated Recording and Application to High Molecular Weight Polystyrene Solutions

Guenther Meyerhoff* and Bernd Appelt

Institut für Physikalische Chemie und Sonderforschungsbereich, SFB 41, Universität Mainz, Jakob-Welder-Weg 15, D-6500 Mainz, West Germany. Received March 28, 1979

ABSTRACT: A new type of shear gradient viscometer with automated recording of the time of fluid equilibration in a U-shaped capillary is introduced. Comparative measurements with a Zimm-Crothers-type viscometer were in good agreement. The Kuhn-Mark-Houwink relationships were established for extremely high molecular weight polystyrenes of up to $M_w = 40 \times 10^6$ in toluene at 20 °C and in THF at 25 °C and were found to be linear over the entire observed range of molecular weights.

Measuring the viscosity of a polymer or its solutions is an important and convenient method of investigation of polymer characteristics. The possibilities and advantages of this method over others have been discussed elsewhere.¹

The intrinsic viscosity is defined as:

$$[\eta] = \lim_{\substack{c \rightarrow 0 \\ G \rightarrow 0}} \frac{\eta_{1,2} - \eta_1}{\eta_1 c}$$

where η_1 and $\eta_{1,2}$ are the viscosities of the pure solvent and the solution, c is the concentration, and G is the shear gradient. While the extrapolation of the concentration to $c = 0$ is easily achieved, the extrapolation to $G = 0$ poses some difficulties. Commonly, for polymers at low concentrations, the shear dependence can be neglected as long as the molecular weight is not very high. For polystyrene in good solvents, it has been shown¹ that up to $[\eta] = 500$ mL/g or $M_w = 2 \times 10^6$ g/mol, the influence of the shear gradient is negligible in most cases. Deviations from the Newtonian behavior arise when polymers of higher molecular weights are investigated.

Two choices exist for determining the limiting viscosity number since the functional dependence of η on G is not clearly established: (a) measuring at very low rates of shear, $G \approx 0$ s⁻¹; and (b) measuring $\eta = \eta(G)$ over a wide range of G , down to very low G . To that end, several methods are available: (a₁) Couette-type rotation viscometers suspended, e.g., on a torsion band which proved to be less accurate for low viscosities; (a₂) Zimm-Crothers viscometers² with a rotating, floating cylinder; (a₃) an advanced version of (a₂) by Gill and Thomson,³ using only one submerged Cartesian diver for different solvents; (b₁) capillary type viscometers with several measuring bulbs placed vertically above each other which work at fairly high rates of shear; (b₂) viscometers with a U-shaped capillary as shown in Figure 1 (instead of using straight capillaries, the long capillary may also be coiled to take up less space); and (b₃) Ubbelohde viscometers of the type (b₂), which are not feasible yet, apparently due to an insufficiently reproducible efflux of the fluid out of the lower end of the capillary.⁴

Theory

In this paper, an automated version of the viscometer with the U-shaped capillary will be described.

As for all capillary viscometers, the Hagen-Poiseuille equation also holds here:

$$\eta = \frac{\pi r^4 \Delta p}{8 l} \frac{dt}{dV} \quad (1)$$

with l for capillary length, ρ for the density of the solution, and g for acceleration due to gravity.

In our particular viscometer, the effective pressure, Δp , amounts to $\Delta p = 2hg\rho$ (see Figure 1a). The rate of flow, dV/dt , through the "viscosity capillary", with radius r , is easily found through the change of height of one of the menisci in the vertical "volume capillaries", R : $dV/dt = \pi R^2 dh/dt$.

After integration, the viscosity amounts to:

$$\eta = \frac{\rho g r^4 (t - t_0)}{4 l R^2 \ln(h_0/h)} = A \rho \frac{(t - t_0)}{\ln(h_0/h)} \quad (2)$$

An accurate determination of the rate of flow is possible by following the meniscus in the precision bore volume capillaries with a cathetometer as a function of time, t .

The maximum rate of shear in this case is given as:

$$G_{\max} = \frac{4R^2(h_0 - h)}{r^3(t - t_0)} \quad (3)$$

G_{\max} is the apparent wall shear rate. Using the true shear rate for capillaries as given by Rabinowitsch⁵ would not change the values of $[\eta]$ for $G = 0$.

We are therefore able to determine the absolute viscosity of any solution as a function of the rate of shear. If the exact dimensions of the viscometer are not known, calibration with solvents of known viscosity and density will furnish the constant A , after plotting $\ln(h/h_0)$ vs. t , from the slope.

Design of the Automated Viscometer

Since cathetometer measurements over an extended period of time are rather strenuous, an automated viscometer was designed making use of flexible light fibers and light barriers.

The problems in the automation may briefly be outlined as: optical detection of the location of one meniscus in a volume capillary and measurement of the distance and time passed since the previous measurement.

To that end, a typical cathetometer (R. Fuess, Berlin-Steglitz) was modified. The telescopic part of the cathetometer was removed with the exception of its mounting which served to move the light barrier along the volume capillary. The light barrier consisted of two flexible light cables with one end close to the volume capillary and the other end attached to the light source or the detector, respectively. Both detector and lamp are mounted on top of the cathetometer (Figure 1b).

Therefore, a passing meniscus can be detected by this light barrier, or if the axle of the cathetometer is driven by a suitable electric motor (three-phase motor No. ES 2145/2-64, Engel, Wiesbaden, with a gear diminishing the rotation number 1:30), the light barrier can actually search the meniscus.

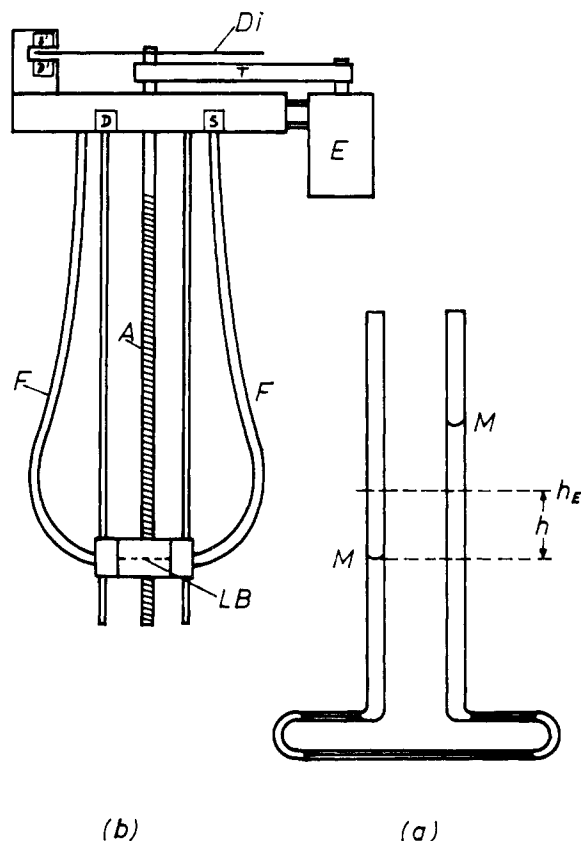


Figure 1. (a) Schematic drawing of the U-shaped capillary viscometer with "viscosity capillary", r , and the precision bore "volume capillary", R . The menisci, M , attain equilibrium at the height $h = h_E$. (b) Schematic drawing of the automated viscometer: The light barrier (LB) consists of two flexible light fibers (F) connecting the light source (S) and the detector (D) with the actual measuring site (and is mounted in reality via a rod extension on the telescopic support of the cathetometer). The axle (A), driven by the electric motor (E) via a transmission (T), moves the light barrier up and down. Attached to the axle is a disk (Di) with 100 precision bore holes which pass light from a source (S') to a detector (D') counting the holes and thus measuring the height h (100 holes = 1/mm). During the measurement the viscometer is held in position by clamps attached to a ringstand placing the left meniscus of Figure 1a in front of the axle between the light barrier.

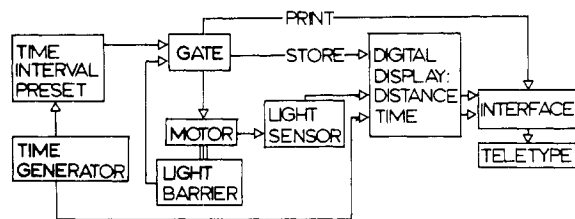


Figure 2. Block diagram of the automated viscometer.

In order to measure the passed distance from the start to the new location of the meniscus, a disk with 100 precision bore holes on its outer diameter is placed on top of the cathetometer's axle. One complete rotation is therefore equivalent to 100 holes which corresponds to 1 mm in height. On rotation of the axle, the light barrier will move up or down while the holes are counted by a light sensor, thus measuring the passed distance.

An electronic timer is started at the beginning of the experiment, and the time is read out whenever the meniscus is reached. The search and detection of the meniscus as well as time and distance computation are executed by an electronic unit, the block diagram of which is shown in Figure 2.

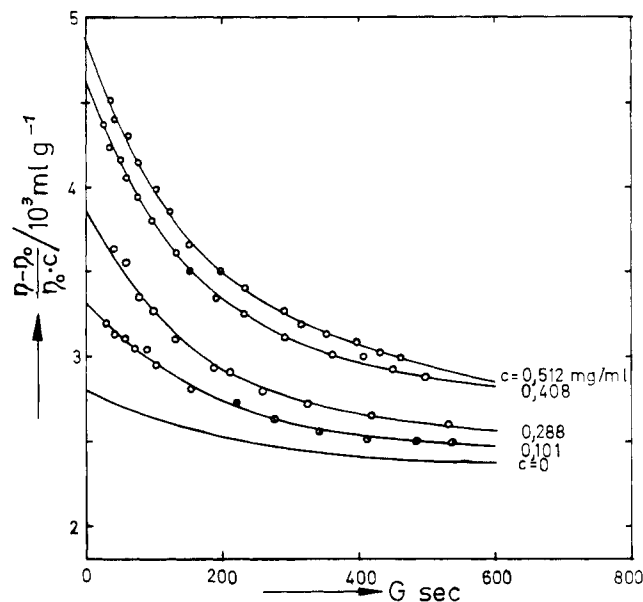


Figure 3. Shear dependence of the reduced viscosity for Th A3-18 in toluene at 20 °C. The lowest line ($C=0$) represents the shear dependence of the viscosity number $[\eta]$.

A typical run will briefly be described as follows: At the beginning of the experiment, the light barrier is in an electronically well-defined position, and the dropping meniscus is in an arbitrary position. A time interval is preset after which the search for the meniscus will begin. The motor will drive the light barrier up (or down) until it reaches the meniscus; the passed time and distance are then displayed digitally as well as printed and punched out by a teletype. At the end of the preset time interval, the search is automatically resumed following the above procedure. This is repeated until the meniscus has become stationary at $h = h_E$, i.e., liquid equilibration is reached. The equilibrium may be repeatedly checked by a manually-triggered search for the meniscus. Results are calculated afterwards with a simple computer program utilizing the punched tape.

Experimental Section

Toluene (p.a., Merck, Darmstadt) and tetrahydrofuran (technical grade, distilled over potassium) were used as solvents.

Anionically prepared polystyrene samples were purchased from Pressure Chemical Co. (Pittsburgh) and Toyo Soda Co. (Tokyo). The thermal polymers and the fractions thereof were prepared by us; details are given elsewhere.⁹

Low molecular weight samples were measured in Ubbelohde viscometers with built-in sinter crucibles for filtering. Two stock solutions of each sample were diluted three times in the viscometer, thus eight different concentrations were measured.

High molecular weight samples were measured in the U-shaped capillary viscometer; some were checked with the Zimm-Crothers viscometer. On the average, five-to-six solutions were prepared and centrifuged for about 1 h at 10000 rpm for purification.

Results and Discussion

Typical results are shown in Figure 3, where the reduced viscosity is plotted as a function of the gradient for different concentrations. For this very high molecular weight polystyrene of $M_w = 35 \times 10^6$, all curves display a pronounced curvature at low shear gradients which decreases with lower concentration, an effect which is still to be found for $[\eta]$ at $c = 0$. Extrapolation to zero shear gradient is easily accomplished due to the many data points.

The limiting viscosity number is obtained by the usual Huggins plot. For the sake of comparison, results also obtained with a Zimm-Crothers viscometer² are shown in

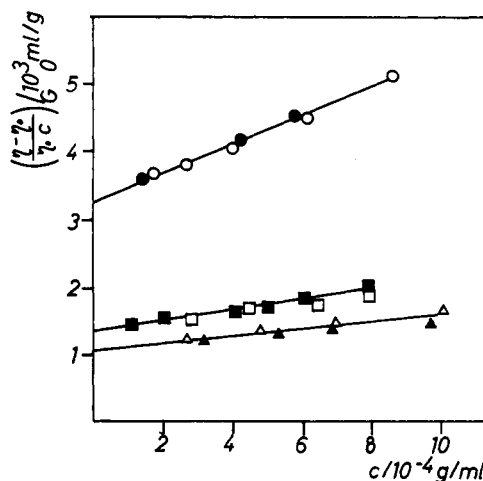


Figure 4. Concentration dependence of the reduced viscosity for (Δ) TSK (7.4×10^6), (◻) TSK (9.5×10^6), and (○) Th A2-18 F2 in toluene at 20 °C as found by the U-shaped capillary viscometer (full symbols) and the Zimm-Crothers viscometer (open symbols).

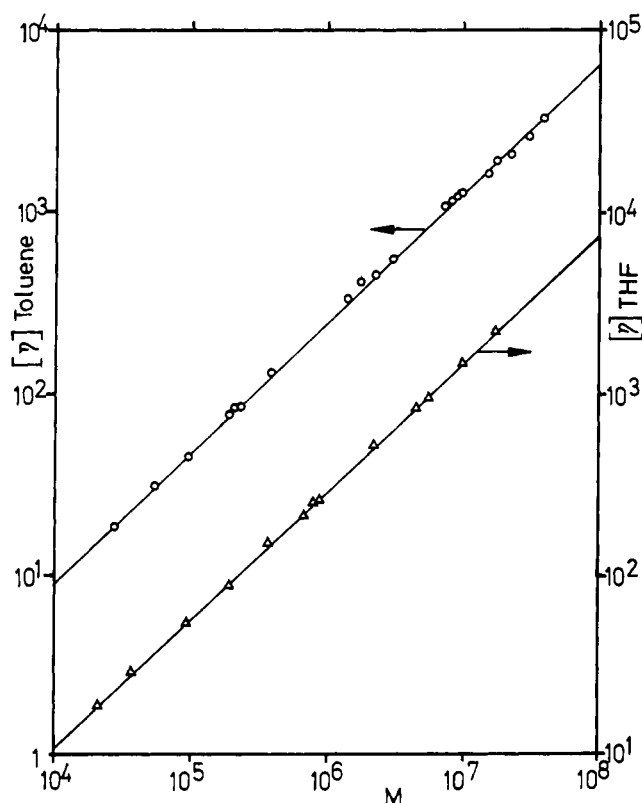


Figure 5. Relation between viscosity number and molecular weight for polystyrene in toluene (○) at 20 °C and THF (Δ) at 25 °C.

Figure 4 and are in good agreement, especially considering that even different capillary viscometers of the same type may give slightly different Huggins constants.

Our viscometer has, therefore, some definite advantages: (a) the functional dependence of η or $(\eta_{1,2} - \eta_1)/\eta_1 c$ on G is obtained over a wide range of shear gradients; and (b) one viscometer may be used for any solvent (also for solvents of low density which raise some problems for viscometers with floating cylinders). An additional advantage is that the viscometer can be replaced by a dilatometer and kinetic measurements of any kind can in this way be automated just as easily.

With our new viscometer, we established the Kuhn-

Table I
Molecular Weights and Limiting Viscosity Numbers of the Polystyrene Samples in Toluene and THF^a

sample	mol wt	mode of prep- aration	[η], g/mL	
			tol- uene (20 °C)	THF (25 °C)
PCC	20 400	anionic		17.3
PCC	37 000	anionic		26.8
PCC	97 200	anionic		48.7
PCC	2.0×10^5	anionic		78.8
PCC	3.9×10^5	anionic	126	134
PCC	6.7×10^5	anionic		189
PCC	8.6×10^5	anionic		244
TSK	1.23×10^6	anionic		309
TSK	2.42×10^6	anionic		498
TSK	2.53×10^6	anionic		521
TSK	2.88×10^6	anionic	525	
TSK	4.59×10^6	anionic		800
TSK	5.55×10^6	anionic		895
TSK	7.40×10^6	anionic	1050	
TSK	9.60×10^6	anionic	1250	1350
TSK	15.2×10^6	anionic	1700	
TSK	18.1×10^6	anionic	1900	2100
Th A 2-18	22.4×10^6	thermal	2050	
Th A 3-18	35.0×10^6	thermal	2800	3220
Th A 4-18	22.7×10^6	thermal	2025	2650
Th A 2-18	39.6×10^6	fraction F2	3275	
Th A 2-18	29.7×10^6	fraction F4	2600	
Th A 2-18	23.4×10^6	fraction F6	2100	
Th A 3-18	9.04×10^6	fraction F3	1250	
Th A 3-18	8.73×10^6	fraction F4	1150	

^a Molecular weights of PCC-TSK = 7.40×10^6 , as given by the supplier TSK = 9.60×10^6 . Th A 3-18 fraction F4 obtained by light scattering.⁹ Suppliers: Pressure Chemical Co., PCC, Pittsburg, Pa.; Toyo Soda Co., TSK, Tokyo.

Mark-Houwink relationships for polystyrene in toluene at 20 °C as

$$[\eta] = 1.069 \times 10^{-2} M^{0.724}$$

and in THF at 25 °C as

$$[\eta] = 1.314 \times 10^{-2} M^{0.714}$$

Both relations were found to be strictly linear over the entire investigated range of molecular weights as can be seen from Figure 5. For clarity, results are also listed in Table I.

For poly(methyl methacrylate) in acetone at 20 °C, which is a good solvent, a linear viscosity-molecular weight log-log relation also holds⁵ for molecular weights up to 40×10^6 .

Our results, however, do not confirm the unexpected data of McIntyre et al.,⁷ who had found a steep increase in the exponent from $a = 0.76$ to $a = 1.2$ for polystyrene in benzene at 30 °C. The examined range of molecular weights was essentially the same ($M_w = 26.8 \times 10^6$ and 43.8×10^6 for McIntyre vs. up to $M_w = 39.6 \times 10^6$ for this work), although the tests were done in slightly different but good solvents; this influence, however, should be negligible. McIntyre's two samples were prepared by anionic polymerizations and displayed their unusual behavior only in the good solvent. Tacticity effects may be ruled out because they should be more pronounced in θ solvents than in good solvents. Also, our anionic samples up to $M_w = 18.1 \times 10^6$ fit the same straight line as the thermally polymerized samples and their fractions, respectively, with M_w up to 39.6×10^6 .⁹ In addition, our samples were investigated with both types of viscometers, giving the same viscosity numbers and resulting in the described Kuhn-Mark-Houwink relations.

Recently, Rosser et al.⁸ reported on a polystyrene prepared by emulsion polymerization with $M_w = 18 \times 10^6$, with a fairly narrow molecular weight distribution, and with $[\eta] = 3150$ for toluene at 20 °C. This would mean the same type of deviation from the linear log–log relation as that claimed by McIntyre.⁷

Any deviation from the linear plot would have to originate from a change in the radius of gyration. Different methods of investigation pertaining to the radius of gyration, such as light scattering ($R^2 \propto M^{1+}$), diffusion ($D \propto M^{-b}$), and sedimentation ($S \propto M^{1-b}$) on the same polystyrene samples of Table I, resulted in typical straight line double logarithmic plots⁹ as can be expected for a thread-like coiling polymer. Considering all of the presented data, it is thought that the results of this work are more reliable than the three viscosity numbers for high molecular weight polystyrene in a good solvent reported elsewhere.^{7,8}

Acknowledgment. The authors are grateful to the Arbeitsgemeinschaft Industrieller Forschungsverbände (AIF) for support of this work, to Mr. Kurt Hartmann for his help in developing the automated viscometer, and to Mrs. Carola Tomalla-Jarzyk for viscosity measurements.

References and Notes

- (1) G. Meyerhoff, *Adv. Polym. Sci.*, **3**, 59 (1961).
- (2) B. H. Zimm, D. Crothers, *Proc. Natl. Acad. Sci. U.S.A.*, **48**, 905 (1962).
- (3) J. Gill, D. Thomsen, *Proc. Natl. Acad. Sci. U.S.A.*, **57**, 562 (1967).
- (4) Unpublished results of our laboratory.
- (5) B. Rabinowitsch, *Z. Phys. Chem., Abt. A*, **145**, 1 (1929).
- (6) M. Stickler and G. Meyerhoff, *Makromol. Chem.*, **179**, 2745 (1978).
- (7) D. McIntyre, L. J. Fetters, and E. Slagowski, *Science*, **176**, 1041 (1972).
- (8) R. W. Rossner, J. L. Schrag, and J. D. Ferry, *Macromolecules*, **11**, 1061 (1978).
- (9) B. Appelt, Ph.D. Thesis, Mainz, 1977.

A Generalized Bead and Spring Model for the Dynamics of DNA in Solution. Application to the Intrinsic Viscosity

Juan J. Freire and José García de la Torre*

Departamento de Química Física, Facultad de Ciencias, Universidad de Extremadura, Badajoz, Spain. Received March 19, 1979

ABSTRACT: A generalized version of the Rouse–Zimm model is applied to the calculation of the intrinsic viscosity of DNA. Some approximations of the model are examined, and some corrections are introduced in the evaluation of the eigenvalues from which the intrinsic viscosity is calculated. The theoretical results are compared with experimental data to obtain the molecular parameters of the model. The statistical segment length so obtained is analyzed together with that extracted from the wormlike chain model and also from experimental data of other macroscopic properties. A first estimation of the excluded volume effects is also discussed.

In the study of chain macromolecules in solution, two different models can be used: the continuous Kratky–Porod¹ wormlike chain and the discrete Rouse–Zimm bead-and-spring model.^{2,3} The former has the great advantage of representing chain stiffness between the limiting cases of flexible coil and rigid rod, while the latter, in its original formulation,³ is only valid for flexible chains. However, the Rouse–Zimm model is, by far, superior to the wormlike chain in the simplicity of the physical concepts and mathematical details embodied in the evaluation of dynamical properties, and, consequently, it is currently considered the most adequate description of the low-frequency dynamics of flexible polymers in solution. In the model, intramolecular motions are represented by a set of relaxation times or equivalent eigenvalues, from which many dynamical properties (intrinsic viscosity,³ quasielastic light scattering,⁴ flow linear dichroism,⁵ etc.) are easily derived.

The above considerations illustrate the potential usefulness of extending the applicability of the Rouse–Zimm model to stiff chains such as DNA, specially if the model parameters can have some molecular interpretations as has been recently suggested by Lin and Schurr.⁶ A first attempt in this direction was made by Simon,⁷ who proposed a generalized version of the model in which chain stiffness is taken into account as a first perturbation by introducing springs connecting second-neighboring beads. Comparison of this model with experimental data of total-intensity light scattering and sedimentation coefficients of high-molecular-weight DNA has been made⁸ and shows that the statistical length predicted by the model is similar to that

obtained for a wormlike chain. For these properties, however, explicit introduction of the relaxation times corresponding to the realistic nondraining limit of hydrodynamic interactions is not needed, and, therefore, the theory has also to be tested with other properties more directly related to the relaxation times.

In the present work, we performed a comparison of the Simon model with existing⁹ experimental data of the intrinsic viscosity of high-molecular-weight DNA. These data (along with others for DNA fragments of lower molecular weight^{10,11}) have been previously interpreted^{12,13} by means of the Yamakawa–Fujii theory^{12,14} that describes the hydrodynamic behavior of a wormlike chain, and, consequently, they seem very adequate to check the theoretical expressions for the eigenvalues derived from the Simon model.

In our revision of the calculations for these eigenvalues, we have arrived at an approximate expression significantly different from that of Simon. We have verified the validity of our new expression by comparing numerical eigenvalues calculated from it with those obtained by exact diagonalization.

The comparison between the revised theory and the experimental data yields values for the two parameters of the model that do not completely agree with those obtained with other properties. This fact is discussed in terms of excluded volume effects, which are larger for the intrinsic viscosity. We have made an estimation of these effects that give a statistical length of DNA close to the one corresponding to an excluded volume wormlike model.^{15–17}